Electronic Supplementary Information

The Revelation of Glucose Adsorption Mechanisms on Hierarchical Metal-Organic Frameworks Using a Surface Plasmon Resonance Sensor

Gilang Gumilar[1,2,3], Silvia Chowdhury[4], Ganes Shukri[2,3], Aep Patah[5], Nugraha Nugraha[2,3], Joel Henzie[6], Isa Anshori[7], Yusuf Valentino Kaneti[4], Brian Yuliarto[2,3]**

[1] *Faculty of Vocational Studies, Institut Teknologi Sains Bandung, Central Cikarang, Bekasi 17530, Indonesia*

[2] *Research Center for Nanoscience and Nanotechnology (RCNN), Institut Teknologi Bandung, Bandung 40132, Indonesia*

[3] *Advanced Functional Materials Research Group, Faculty of Industrial Technology, Institut Teknologi Bandung, Bandung 40132, Indonesia*

[4] *School of Chemical Engineering and Australian Institute for Bioengineering and Nanotechnology (AIBN), The University of Queensland, Brisbane, QLD 4072, Australia*

[5] *Inorganic & Physical Chemistry Research Division, Institut Teknologi Bandung, Bandung 40132, Indonesia*

[6] *International Center for Materials Nanoarchitectonics (WPI-MANA), National Institute for Materials Science (NIMS), 1-1 Namiki, Tsukuba, Ibaraki 305-0044, Japan*

[7] *Lab-on-Chip Group, Biomedical Engineering Department, Institut Teknologi Bandung, Bandung 40132, Indones*ia

E-mails: *gilang.gumilar@itsb.ac.id; brian@itb.ac.id*

S1. Materials and Method

Chemicals

Copper(II) nitrate trihydrate ($Cu(NO_3)_2 \cdot 3H_2O$, 99.5%), manganese(II) nitrate tetrahydrate ($Mn(NO_3)_2 \cdot 4H_2O$, 99.5%), and nickel(II) nitrate hexahydrate ($Ni(NO_3)_2 \cdot 6H_2O$, 99.5%) were purchased from Fujifilm Wako Pure Chemical Corporation (Japan). Zirconium(IV) chloride ($ZrCl_4$, 99.5%) was purchased from Sigma-Aldrich (Japan). The organic linker, benzene-1,4-dicarboxylic acid (BDC), was purchased from Sigma-Aldrich (Japan). The solvents, *N*, *N*-dimethylformamide (DMF), and acetonitrile (C_2H_3N, 99.8%), were purchased from Fujifilm Wako Pure Chemical Corporation (Japan). Polyvinylpyrrolidone K-30 (PVP) (M_w = 40.000), maltose ($C_{12}H_{22}O_{11}$, ≥ 99%), and L-ascorbic acid ($C_6H_8O_6$, 99%) were purchased from Nacalai Tesque (Japan). Uric acid ($C_5H_4N_4O_3$, ≥ 99%) and urea (CH_4N_2O) were purchased from Sigma-Aldrich (Japan). Phosphate buffer saline (PBS, pH 7.4) was made in our laboratory (using 0.137 M NaCl, 0.0027 M KCl, 0.01 M Na_2HPO_3, and 0.0018 M KH_2PO_4). Sigma-Aldrich, Singapore provided the commercial human serum (derived from male AB clotted whole blood).

Fabrication of hierarchical 3D sheet/plate like M-BDC (M = Cu, Mn, Ni, and Zr)

The hierarchical sheet-/plate-like M-BDC samples were synthesized according to our previous work with slight modifications.[1] First, two types of solutions were prepared. Solution A was made by dissolving 0.3 g of the metal precursor in 10 mL of DMF and 30 mL of acetonitrile (ACN). Meanwhile, solution B was prepared by dissolving 0.3 g of BDC in 30 mL of DMF and 10 mL of ACN, followed by the addition of PVP using a BDC/PVP mass ratio of 1:3 for Cu-BDC and Ni-BDC and 1:5 for Mn-BDC and Zr-BDC under stirring. In the next step, 4 mL of solution A and 4 mL of solution B were mixed in a 50 mL vial and sonicated for 2 min. The synthesis process was performed in an oil bath at 135 °C for 24 h without stirring. The resulting precipitate was then centrifuged at 14000 rpm for 8 minutes and washed with DMF, ethanol, and methanol three times each. After that, the product was dried overnight in a vacuum oven at 60 °C. Prior to characterization, all samples were activated by dispersing them on chloroform for 24 h, followed by centrifugation and subsequent drying at 120 °C in a vacuum oven overnight. A schematic illustration depicting the general synthesis process of the M-BDC MOFs is given in **Fig. S1**.

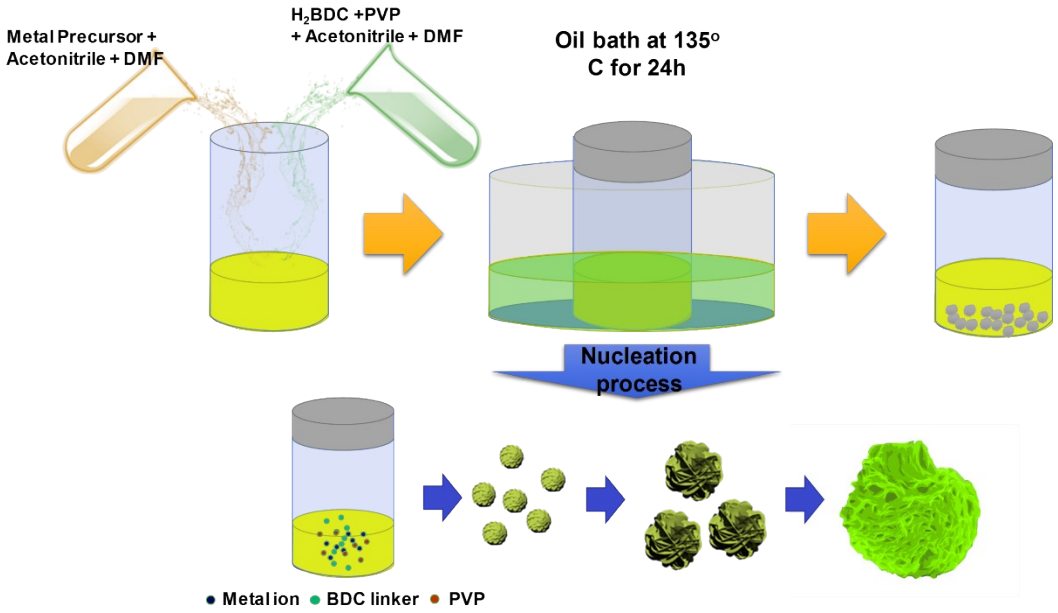

Fig. S1. Schematic diagram showing the solvothermal fabrication of the hierarchicalM-BDC MOFs.

Functionalization of SPR sensor chips with M-BDC MOFs

First, the standard SPR sensor chip (20 x 20 mm) with a refractive index of 1.61 (consisting of evaporated 5 nm Cr and 45 nm Au film on the Swiss glass) was cleaned by immersing it in piranha solution (H_2SO_4:H_2O_2 volume ratio = 3:1) for 30 s, followed by rinsing with tap water, soapy water, ethanol, and distilled water, respectively, and subsequent drying using air duster gun. The preparation of M-BDC suspension was conducted by dispersing 5 mg of each M-BDC into 5 mL of DMF, followed by sonication for 30 min. The deposition of M-BDC onto the sensor chip surface was carried out by the spin coating method. Typically, 200 µL of the M-BDC suspension was dropped on the substrate and then rotated with an initial speed of 750 rpm for 10 s and a subsequent speed of 2000 rpm for 20 s, followed by drying at 140 °C. The spin coating process was repeated three times with the same parameters for each M-BDC MOF.

Adsorption isotherm studies

Table S1. The two-parameter (Langmuir, Freundlich, Jovanovic, Temkin, and Dubinin-Radushkevich) and three-parameter (Langmuir-Freundlich, Vieth-Sladek, Brouers-Sotolongo, Redlich-Peterson, and Toth) adsorption isotherm models and the corresponding equations in non-linear forms.

Two-parameter equations			**Three-parameter equations**		
Adsorption isotherm model	Non-linear		Adsorption isotherm model	Non-linear	
Langmuir	$\Delta\theta_e = \frac{\Delta\theta_m K_L C_e}{1 + K_L C_e}$	(1)	***Langmuir-Freundlich (Sips)***	$\Delta\theta_e = \frac{\Delta\theta_m (K_{LF} C_e)^{M_{LF}}}{1 + (K_{LF} C_e)^{M_{LF}}}$	(6)
Freundlich	$\Delta\theta_e = K_F C_e^{\,1/n_F}$	(2)	***Vieth-Sladek***	$\Delta\theta_e = K_{VS} C_e + \left(\frac{\Delta\theta_m \beta_{VS} C_e}{1 + \beta_{VS} C_e}\right)$	(7)
Jovanovic	$\Delta\theta_e = \Delta\theta_m\left(1 - e^{(K_J C_e)}\right)$	(3)	***Brouers-Sotolongo***	$\Delta\theta_e = \Delta\theta_m\,(1 - exp\left[-K_{BS}(C_e)^{\alpha}\right]$	(8)
Temkin	$\Delta\theta_e = B_T \ln(A_T C_e)$	(4)	***Redlich-Peterson***	$\Delta\theta_e = \frac{A_{RP} C_e}{1 + B_{RP} C_e^{\,g}}$	(9)
Dubinin-Radushkevich	$\Delta\theta_e = \Delta\theta_m\, exp\left\{-A_D\left[\ln\left(1 + \frac{1}{C_e}\right)\right]^2\right\}$	(5)	***Toth***	$\Delta\theta_e = \Delta\theta_m C_e (b_{To} + C_e^{\,n_{To}})^{1/n_{To}}$	(10)

$\Delta\theta_m$ is maximum adsorption capacity; K_L is Langmuir constant; K_F, n_F are Freundlich constants; K_J is Jovanovic constant; B_T is Temkin isotherm energy constant; A_T is the Temkin isotherm constant; A_D relates to the mean sorption free energy per mole of the sorbate; K_{LF} is the equilibrium constant for heterogeneous solid; M_{LF} is heterogeneous parameters; K_{VS}, β_{VS} are Vieth-Sladek constants; K_{BS}, α are Brouers-Sotolongo constants; A_{RP}, B_{RP}, g are Redlich-Peterson constants; b_{To}, n_{To} are Toth constants; and C_e is glucose concentration in equilibrium.

Adsorption kinetic studies

The models used to predict the glucose adsorption mechanisms on M-BDC were pseudo-first-order, pseudo-second-order, Elovich, and Avrami models with non-linear regression methods. In the pseudo-first-order kinetic adsorption model, the determination of the adsorption rate of the adsorbent is based on the adsorption capacity, while the pseudo-second-order model reflects an adsorption process that is controlled by chemisorption involving valence forces through the sharing of electrons or exchange between the solvent and the adsorbate.[2] The Elovich adsorption kinetic model is frequently used to analyze the adsorption process on heterogeneous surfaces with

reasonable results. Moreover, this model is also able to identify the number of sites and the quantity of adsorption.[3-5] In comparison, the Avrami adsorption kinetic model is used to determine specific changes in kinetic parameters as the adsorption rate is affected by the initial concentration and adsorption time.[2, 5]

Table S2. The non-linear equations for pseudo-first-order, pseudo-second-order, Elovich, and Avrami adsorption kinetic models.

Adsorption kinetic model	Non-linear equation	
Pseudo-first order	$\Delta\theta_t = \Delta\theta_e\,(1 - exp[-k_1 t]$	(11)
	$h_o = k_1 \Delta\theta_e$	(12)
Pseudo-second order	$\Delta\theta_t = \frac{\Delta\theta_e{}^2 k_2 t}{1 + k_2 \Delta\theta_e t}$	(13)
	$h_o = k_2 \Delta\theta_e{}^2$	(14)
Elovich	$\Delta\theta_t = \frac{1}{\beta}\ln(\alpha\beta) + \frac{1}{\beta}\ln(t)$	(15)
Avrami	$\Delta\theta_t = \Delta\theta_e\left\{1 - exp\left[-(k_{AV}t)\right]^{n_{AV}}\right\}$	(16)

k_1 is the rate constant for the pseudo-first-order adsorption; k_2 is the rate constant for the pseudo-second-order adsorption; h_o is the initial adsorption rate; α is the Elovich initial adsorption rate; β is the Elovich adsorption constant; and k_{AV}, n_{AV} are the Avrami constants.

Selectivity and Reusability

To obtain the selectivity coefficient of hierarchical plate-like Zr-BDC in the presence of interfering compounds, the measured response (ΔR) from the equation used by Sarikaya *et al.*[6] was modified by the angular change $\Delta\theta$ using the equation is expressed below:

$$k = \frac{\Delta\theta_{template}}{\Delta\theta_{competitor}} \quad (17)$$

where k is the selectivity coefficient, $\Delta\theta_{template}$ is the angular change in the main biomolecule (glucose), and $\Delta\theta_{competitor}$ is the angular change of the interfering compounds. Then, the reusability of the Zr-BDC-functionalized SPR sensor was quantified by measuring the percentage of the response after n^{th} repetition compared to the first or initial response. The equation used is as follows:

$$\%\, response\ after\ n^{th}\ repetition = \frac{\Delta\theta_{n^{th}\ measurement}}{\Delta\theta_{first\ measurement}} \times 100\% \quad (18)$$

S2. Isotherm Data Analysis

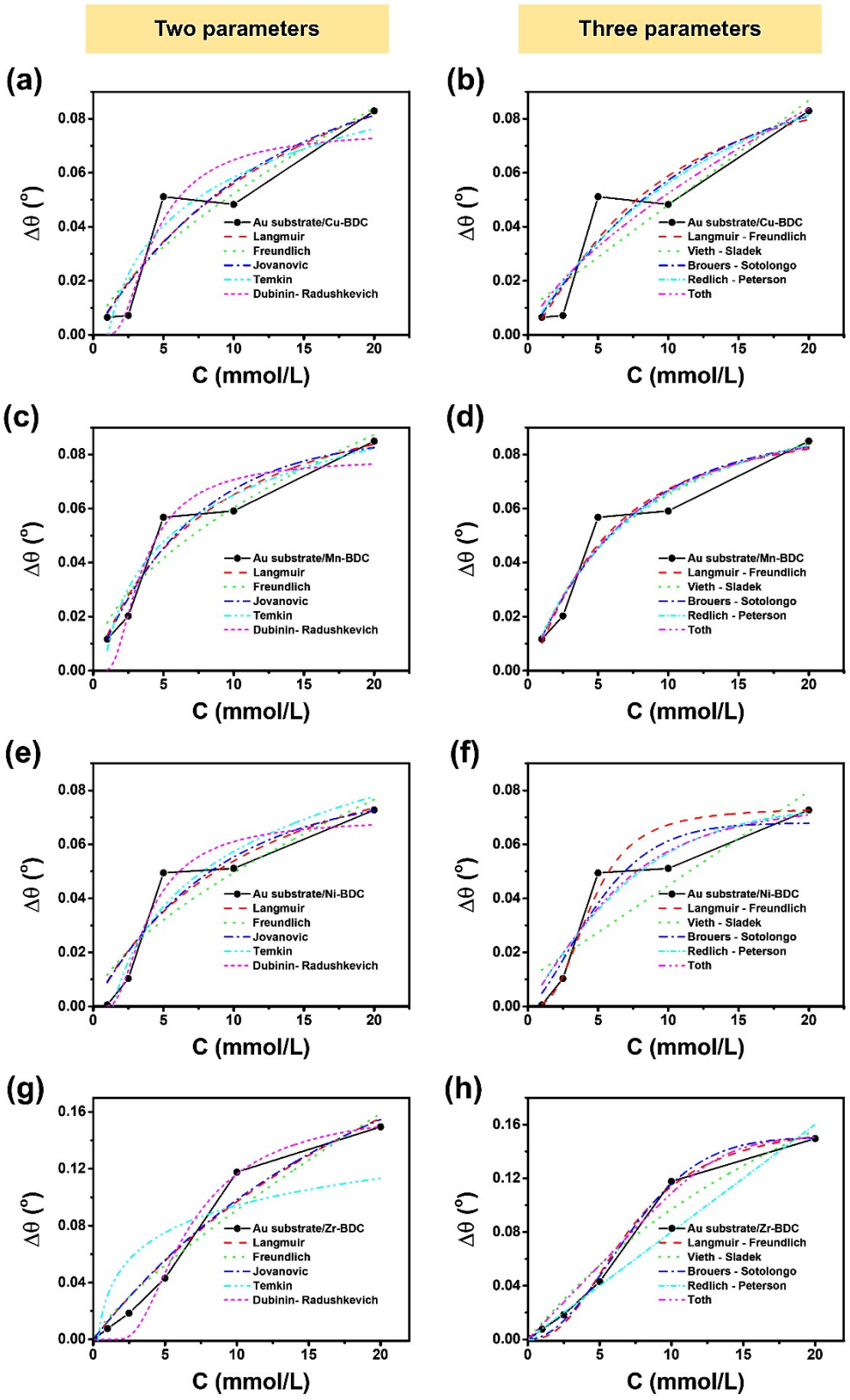

Fig. S2. Non-linear regression curves of two- and three-parameter adsorption isotherm models for glucose adsorption by M-BDC: (a) Cu-BDC (two-parameter model), (b) Cu-BDC (three-parameter model), (c) Mn-BDC

(two-parameter model), (d) Mn-BDC (three-parameter model), (e) Ni-BDC (two-parameter model), (f) Ni-BDC (three-parameter model), (g) Zr-BDC (two-parameter model), and (h) Zr-BDC (three-parameter model).

Table S3. The constants of two parameters adsorption isotherm models and the correlation coefficients for the adsorption of glucose molecules on M-BDC MOFs.

MOF	Langmuir	Freundlich	Jovanovic	Temkin	Dubinin-Radushkevich
Cu-BDC	[a] $\Delta\theta_m$ = 0.14982 [b] K_L = 0.0597 R^2 = 0.88289	[c] K_F = 0.01084 [d] n_F = 1.46376 R^2 = 0.86919	$\Delta\theta_m$ = 0.09985 [e] K_J = -0.08399 R^2 = 0.88172	[f] A_T = 0.94709 [g] B_T = 0.02595 R^2 = 0.86898	$\Delta\theta_D$ = 0.0758 [h] A_D = 17.33031 [i] R^2 = 0.88149
Mn-BDC	$\Delta\theta_m$ = 0.11757 K_L = 0.12429 R^2 = 0.93578	K_F = 0.01762 n_F = 1.87102 R^2 = 0.90585	$\Delta\theta_m$ = 0.08724 K_J = -0.14668 R^2 = 0.93351	A_T = 1.35022 B_T = 0.02496 R^2 = 0.93321	$\Delta\theta_D$ = 0.07863 A_D = 11.66969 R^2 = 0.90459
Ni-BDC	$\Delta\theta_m$ = 0.11595 K_L = 0.08669 R^2 = 0.89177	K_F = 0.01161 n_F = 1.58789 R^2 = 0.84975	$\Delta\theta_m$ = 0.08018 K_J = -0.11705 R^2 = 0.89626	A_T = 0.70272 B_T = 0.0294 R^2 = 0.78055	$\Delta\theta_D$ = 0.06962 A_D = 14.54861 R^2 = 0.95091
Zr-BDC	$\Delta\theta_m$ = 0.39491 K_L = 0.03253 R^2 = 0.96077	K_F = 0.01432 n_F = 1.24441 R^2 = 0.94584	$\Delta\theta_m$ = 0.2312 K_J = -0.05531 R^2 = 0.96301	A_T = 3.06109 B_T = 0.02755 R^2 = 0.6959	$\Delta\theta_D$ = 0.16388 A_D = 37.77964 R^2 = 0.98282

[a] $\Delta\theta_m$ or $\Delta\theta_D$ = maximum adsorption capacity; [b] K_L = Langmuir constant; [c] K_F, [d] n_F = Freundlich constants; [e] K_J = Jovanovic constant; [f] A_T = Temkin isotherm constant; [g] B_T = Temkin isotherm energy constant; [h] A_D = mean sorption free energy per mole of the sorbate, and [i] R^2 = correlation coefficient.

Table S4. The constants of three-parameter adsorption isotherm models and the corresponding correlation coefficients for the adsorption of glucose molecules by M-BDC MOFs.

MOF	Langmuir-Freundlich	Vieth-Sladek	Brouers-Sotolongo	Redlich-Peterson	Toth
Cu-BDC	[a] $\Delta\theta_m$ = 0.10432	$\Delta\theta_m$ = 0.00941	$\Delta\theta_m$ = 0.09553	[h] A_{RP} = 0.00874	$\Delta\theta_m$ = 2.1 x 10^{11}
	[b] K_{LF} = 0.12146	[d] K_{VS} = 0.00387	[f] K_{BS} = 0.08316	[i] B_{RP} = 0.0497	[k] b_{To} = 2.32609
	[c] M_{LF} = 1.32515	[e] B_{VS} = 6 x 10^{45}	[g] α = 1.04137	[j] g = 1.04813	[l] n_{To} = 0.03929
	R^2 = 0.8867	R^2 = 0.83347	R^2 = 0.8819	R^2=0.88293	[m] R^2 = 0.8702
Mn-BDC	$\Delta\theta_m$ = 0.09717	$\Delta\theta_m$= 0.11757	$\Delta\theta_m$ = 0.08837	A_{RP} = 0.01365	$\Delta\theta_m$ = 0.09966
	K_{LF} = 0.18805	K_{VS} = 1.93x10^{-18}	K_{BS} = 0.14921	B_{RP} = 0.08837	b_{To} = 16.65548
	M_{LF} = 1.28131	B_{VS} = 0.12429	α = 0.97508	g = 1.08444	n_{To} = 1.35679
	R^2 = 0.93964	R^2 = 0.93578	R^2 = 0.93361	R^2 = 0.9362	R^2 = 0.93718
Ni-BDC	$\Delta\theta_m$ =0.07345	$\Delta\theta_m$ = 0.01002	$\Delta\theta_m$ = 0.06789	A_{RP} = 0.00828	$\Delta\theta_m$ = 0.07669
	K_{LF} = 0.22405	K_{VS} = 0.00348	K_{BS} = 0.07431	B_{RP} = 0.01368	b_{To} = 155.16221
	M_{LF} = 2.95308	B_{VS} = 2.1x10^{34}	α = 1.49627	G = 1.52343	n_{To} = 2.23255
	R^2 = 0.99879	R^2 = 0.77925	R^2 = 0.91244	R^2 = 0.90011	R^2 = 0.90367
Zr-BDC	$\Delta\theta_m$ = 0.16299	$\Delta\theta_m$=0.39483	$\Delta\theta_m$ = 0.15067	A_{RP} = 0.00801	$\Delta\theta_m$ = 0.15194
	K_{LF} = 0.14116	K_{VS}=3.4x10^{-17}	K_{BS} = 0.01614	B_{RP} = 1.8x10^{-4}	b_{To} = 7.7x10^{7}
	M_{LF} = 2.45169	B_{VS}=0.03254	α = 1.95791	g = -14.47696	n_{To} = 6.9315
	R^2 = 0.99324	R^2=0.96077	R^2 = 0.99643	R = 0.92119	R^2 = 0.98347

[a] $\Delta\theta_m$ = maximum adsorption capacity; [b] K_{LF} = Equilibrium constant for heterogeneous solid; [c] M_{LF} = Heterogeneous parameters; [d] K_{VS}, [e] β_{VS} = Vieth-Sladek constants; [f] K_{BS}, [g] α = Brouers-Sotolongo constants; [h] A_{RP}, [i] B_{RP}, [j] g = Redlich-Peterson constants; [k] b_{To}, [l] n_{To} = Toth constants, and [m] R^2 = correlation coefficient.

Notes for Fig. S2, Table S1, and Table S2:

(I) Adsorption isotherm analysis for Cu-BDC

The non-linear regression curves of the two-parameter and three-parameter adsorption isotherm models for glucose adsorption by Cu-BDC are given in **Fig. S2a** and **S2b**, respectively. For the two-parameter isotherm model, the parameters are shown in **Table S3**. The highest correlation coefficient is shown by the Langmuir model (R^2 = 0.88289) with $\Delta\theta_m$ = 0.14982 mmol/g. In comparison, for the three-parameter model, the largest correlation coefficient is obtained using the Langmuir-Freundlich model (R^2 = 0.8867) with $\Delta\theta_m$ = 0.10432 mmol/g, followed by Redlich-Peterson (R^2 = 0.88293), Langmuir (R^2 = 0.88289), Brouers-Sotolongo (R^2 = 0.8819), Jovanovic (R^2 = 0.88172), Dubinin-Radushkevich (R^2 = 0.88149), Toth (R^2 = 0.8702), Freundlich (R^2 = 0.8702), Temkin (R^2 = 0.86898), and Vieth-Sladek (R^2 = 0.83347). Further, the $\Delta\theta_m$ value follows the order of Toth > Langmuir > Langmuir-Freundlich > Jovanovic > Brouers-Sotolongo > Dubinin-Radushkevich > Vieth-Sladek. Based on the R^2 value, the glucose adsorption process by Cu-BDC follows the Langmuir-Freundlich model.

According to the Langmuir-Freundlich adsorption model, the distribution of adsorption energy occurs on a heterogeneous surface where the adsorbate adsorption with high concentration becomes the Langmuir isotherm model and, at low concentration, the adsorption mechanism becomes the Freundlich model.[7] The Freundlich model determines the adsorption process with the adsorbate binding mechanism on a multilayer site, whereas the Langmuir model assumes binding at a homogeneous binding site.[6] The $\Delta\theta_m$ value for the Langmuir-Freundlich isotherm model (0.10432 mmol/g) is slightly smaller than the $\Delta\theta_m$ value for the Langmuir model (0.14982 mmol/g) with an affinity constant (K_{LF}) of 0.12146 mmol/L. The heterogeneous parameter value of the Langmuir-Freundlich isotherm model (M_{LF}) is 1.3251. If the M_{LF} value is > 1, there is a cooperative reaction between a sorption site and n sorbate molecules and the K_{LF} value is the affinity constant of the reaction. This is similar to the Hill model, where there is a cooperative interaction of the ligand molecules with the macromolecules, meaning that the adsorbate has the ability to bind at one site on the adsorbent, which in turn, affects other binding sites on the same adsorbent (binding of different species on a homogeneous layer).[8, 9] This phenomenon occurs during the binding process of glucose by Cu-BDC which competes with the hydrolysis of water molecules with Cu−O−C group in Cu-BDC.

(II) Adsorption isotherm analysis for Mn-BDC

The non-linear fitting of adsorption isotherm models for glucose-Mn-BDC system is shown in **Fig. S2c** and **S2d**. The correlation coefficient of each model shows the non-linear regression fitting accuracy to the experimental data, as shown in **Table S3** and **Table S4.** For glucose adsorption by Mn-BDC, the highest correlation coefficient value is obtained by the Langmuir-Freundlich model with an R^2 value of 0.93964, but the R^2 values for other models are not that much different. Based on the order from highest to smallest, the correlation coefficient value

of each model is as follows: Langmuir-Freundlich (R^2 = 0.93964) > Toth (R^2 = 0.93718) > Redlich-Peterson (R^2 = 0.9362)> Langmuir and Vieth-Sladek (R^2 = 0.93578) > Brouers-Sotolongo (R^2 = 0.93361) > Jovanovic (R^2 = 0.93351) > Temkin (R^2 = 0.93321)> Freundlich (R^2 = 0.90585) > Dubinin-Radushkevich (R^2 = 0.90459). Furthermore, the maximum adsorption capacity parameters follow the order of Langmuir = Vieth-Sladek ($\Delta\theta_m$ = 0.11757 mmol/g) > Toth ($\Delta\theta_m$ = 0.09966 mmol/g) > Langmuir-Freundlich ($\Delta\theta_m$ = 0.09717 mmol/g) > Brouers-Sotolongo ($\Delta\theta_m$ = 0.08837 mmol/g) > Jovanovic ($\Delta\theta_m$ = 0.08724 mmol/g) > Dubinin-Radushkevich ($\Delta\theta_D$ = 0.07863 mmol/g).

The adsorption isotherm process on the detection of glucose using Mn-BDC functionalized SPR sensor chip is conformable to the Langmuir-Freundlich model and shows similarity to the glucose adsorption mechanism by Cu-BDC. In the Langmuir-Freundlich model, the isotherm parameters are $\Delta\theta_m$ = 0.09717 mmol/g, M_{LF} = 1.28131, and K_{LF} is 0.18805 mmol/L. These values reflect the binding of other molecules during the glucose adsorption process, in this case is the water molecules, because the M_{LF} value is greater than 1. These values indicate that cooperative interactions between glucose and the Cu-BDC sample follow the adsorption mechanism described in the Hill adsorption isotherm model.

(III) Adsorption isotherm analysis for Ni-BDC

The dynamic responses of glucose-Ni-BDC interactions were evaluated using adsorption isotherm with a non-linear regression method, as shown in **Fig. S2e** and **S2f**, two and three parameters, respectively. The obtained parameters and correlation coefficients from the analysis are given in **Table S3** and **Table S4.** From these Tables, the highest correlation coefficient R^2 is obtained from the Langmuir-Freundlich model with R^2 = 0.99879. The R^2 values for the other models follow the order of Langmuir-Freundlich (R^2 = 0.99879) > Dubinin-Radushkevich (R^2 = 0.95091) > Brouers-Sotolongo (R^2 = 0.91244) > Toth (R^2 = 0.90367) > Redlich-Peterson (R^2 = 0.90011) > Jovanovic (R^2 = 0.89626) > Langmuir (R^2 = 0.89177) > Freundlich (R^2 = 0.84975) > Temkin (R^2 = 0.78055) > Vieth-Sladek (R^2 = 0.77925). In comparison, the maximum adsorption capacity values follow the order of Langmuir ($\Delta\theta_m$ = 0.11595 mmol/g) > Jovanovic ($\Delta\theta_m$ = 0.08018 mmol/g) > Toth ($\Delta\theta_m$ = 0.07669 mmol/g) > Langmuir-Freundlich ($\Delta\theta_m$ = 0.07345 mmol/g) > Dubinin-Radushkevich ($\Delta\theta_D$ = 0.06962 mmol/g) > Brouers-Sotolongo ($\Delta\theta_m$ = 0.06789 mmol/g) > Vieth-Sladek ($\Delta\theta_m$ = 0.01002 mmol/g).

Based on the correlation coefficient data, the glucose adsorption by Ni-BDC follows the Langmuir-Freundlich model with isotherm parameters of $\Delta\theta_m$ = 0.07345 mmol/g, M_{LF} = 2.95308, and K_{LF} = 0.22405 mmol/L. According to this model, if the M_{LF} value > 1, the adsorption mechanism follows the Hill adsorption isotherm model, where the glucose binding process occurs through cooperative interactions. Similarly, as Cu-BDC and Mn-BDC, the interaction process involves one homogeneous adsorbent and different species. The dynamic response curve for glucose detection by Ni-BDC shows a decreasing trend in the SPR signal at the beginning (baseline determination) when glucose solution is driven to the PBS flow up to a concentration of 1

mmol/L. At such low concentrations, the hydrolysis process likely dominates over the glucose binding process by Ni-BDC, which coincides in time. However, after driving 2.5 mmol/L glucose, the SPR signal gradually increases with increasing concentration as expected. This observation indicates that the adsorption process of glucose by Ni-BDC becomes dominant over the hydrolysis of Ni-BDC.

(IV) Adsorption isotherm analysis for Zr-BDC

The dynamic response of Zr-BDC to glucose was analyzed using both two- and three-parameter isotherm models and the corresponding non-linear regression curves are depicted in **Fig.s S2g** and **S2h**, respectively. From this curve, the isotherm parameters are obtained, as summarized in **Table S3** and **Table S4**, which can be used to predict the adsorption mechanism that occurs during the detection process and the accuracy of such prediction. For Zr-BDC, the highest correlation coefficient is achieved by the Brouers-Sotolongo model with an R^2 value of 0.99643. Therefore, it can be assumed that the glucose adsorption process by Zr-BDC resembles the adsorption mechanism of this model. The correlation coefficient values of the other models are, in descending order: Brouers-Sotolongo (R^2 = 0.99643) > Langmuir-Freundlich (R^2 = 0.99324) > Toth (R^2 = 0.98347) > Dubinin-Radushkevich (R^2 = 0.98282) > Jovanovic (R^2 = 0.96301) > Langmuir = Vieth-Sladek (R^2 = 0.96077) > Freundlich (R^2 = 0.94584) > Redlich-Peterson (R^2 = 0.92119) > Temkin (R^2 = 0.6959). In addition, the $\Delta\theta_m$ value, which indicates the maximum adsorption capacity follows the order of: Langmuir ($\Delta\theta_m$ = 0.39491 mmol/g) > Vieth-Sladek ($\Delta\theta_m$ = 0.39483 mmol/g) > Jovanovic ($\Delta\theta_m$ = 0.2312 mmol/g) > Dubinin-Radushkevich ($\Delta\theta_m$ = 0.16388 mmol/g) > Langmuir-Freundlich ($\Delta\theta_m$ = 0.16299 mmol/g) > Toth ($\Delta\theta_m$ = 0.15194 mmol/g) > Brouers-Sotolongo ($\Delta\theta_m$ = 0.15067 mmol/g).

The mechanism of glucose adsorption by Zr-BDC follows the Brouers-Sotolongo model. In this model, the interaction process that occurs has high heterogeneity by considering a pattern of sorption energy distribution.[10] The high heterogeneity of the Zr-BDC surface in glucose adsorption can be identified from the value of exponent α, where the greater the value, the higher the heterogeneity. The α value is a decent criterion to illustrate the fractal characteristics of heterogeneous surfaces and can also explain the corresponding biosorption mechanisms.[10-12] As shown in **Table S4,** the obtained exponent α value from the non-linear regression analysis is 1.95791. If the exponent $\alpha > 1$, the adsorption process is a slow initial biosorption kinetics process so the active sites would have dissimilar energy.[10] Therefore, the adsorption mechanism of glucose by Zr-BDC is a biosorption with a slow initial sorption.

S3. Kinetic Data Analysis

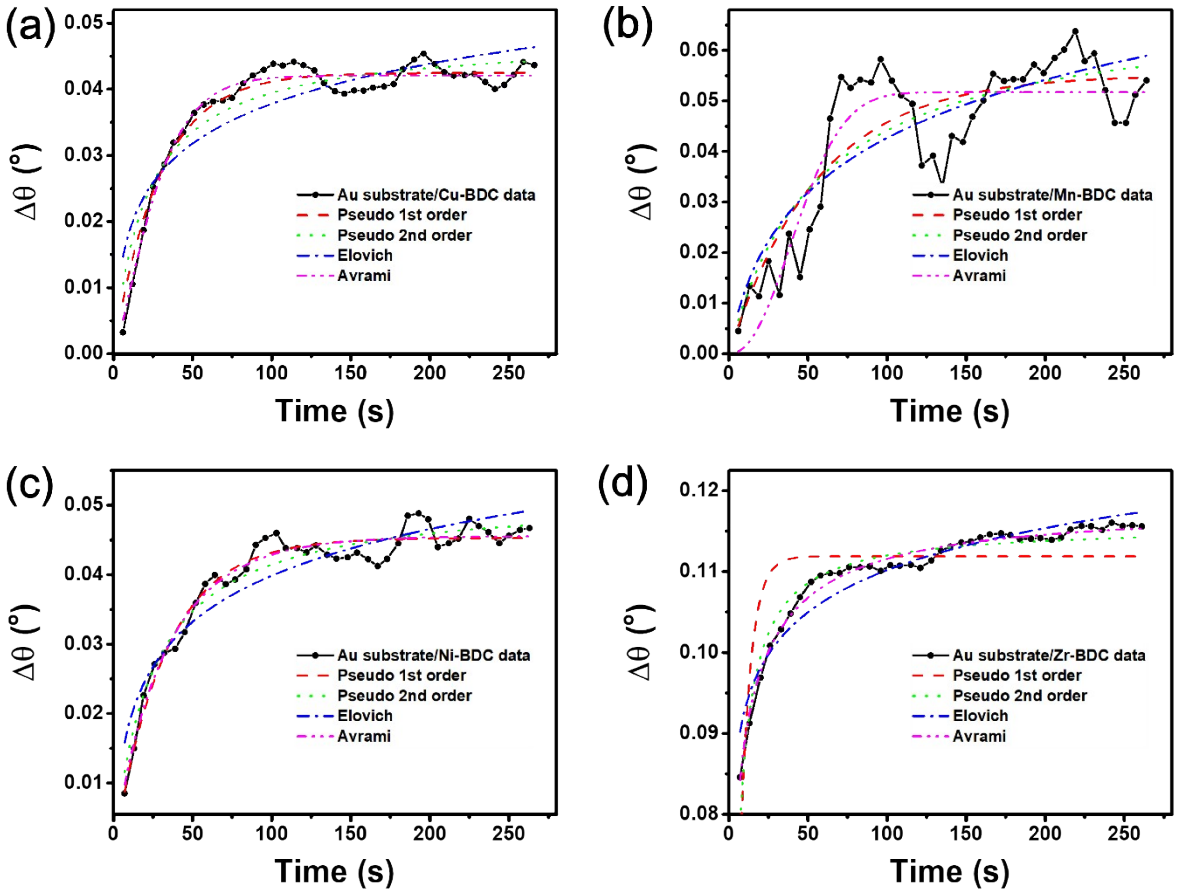

Fig. S3. Non-linear regression curves of the adsorption kinetic models for glucose adsorption by SPR chip sensors functionalized with (a) Cu-BDC, (b) Mn-BDC, (c) Ni-BDC, and (d) Zr-BDC.

Table S5. The parameters and correlation coefficients were obtained from the non-linear regression curves of the adsorption kinetic models for the dynamic responses of M-BDC MOFs towards glucose at a concentration of 10 mmol/L.

M-BDC MOF	Pseudo first-order	Pseudo second- order	Elovich	Avrami
Cu-BDC	[a] $\Delta\theta_e$ = 0.04251 [b] k_1 = 0.03451 R^2 = 0.95515	$\Delta\theta_e$ = 0.04782 [c] k_2 = 0.98663 R^2 = 0.89961	[d] β = 113.20595 [e] α = 0.0063 R^2 = 0.78495	$\Delta\theta_e$ = 0.04207 [f] K_{AV} = 0.01291 [g] n_{AV} = 1.28621 [h] R^2 = 0.96849
Mn-BDC	$\Delta\theta_e$ = 0.05516 k_1 = 0.01771 R^2 = 0.75389	$\Delta\theta_e$ = 0.06909 k_2 = 0.25662 R^2 = 0.73463	β = 56.18971 α = 0.00178 R^2 = 0.70694	$\Delta\theta_e$ = 0.05176 K_{AV} = 1.712x10^{-4} n_{AV} = 2.198 R^2 = 0.78500
Ni-BDC	$\Delta\theta_e$ = 0.04527 k_1 = 0.03083 R^2 = 0.95461	$\Delta\theta_e$ = 0.05146 k_2 = 0.80513 R^2 = 0.94477	β = 10211052 α = 0.00563 R^2 = 0.8806	$\Delta\theta_e$ = 0.04556 K_{AV} = 0.03987 n_{AV} = 0.92541 R^2 = 0.95603
Zr-BDC	$\Delta\theta_e$ = 0.11189 k_1 = 0.15397 R^2 = 0.62608	$\Delta\theta_e$ = 0.11563 k_2 = 2.66488 R^2 = 0.94626	β = 133.32513 α = 179.79905 R^2 = 0.92796	$\Delta\theta_e$ = 0.11708 K_{AV} = 0.66681 n_{AV} = 0.3307 R^2 =0.98447

[a] $\Delta\theta_e$ = adsorption capacity [b] k_1 = Rate constant for the pseudo-first order adsorption; [c] k_2 = Rate constant for the pseudo-second order adsorption; [d] α = Elovich initial adsorption rate; [e] β = Elovich adsorption constant; [f] k_{AV}, [g] n_{AV} = Avrami constants, and [h] R^2 = correlation coefficient.

S4. Calibration Curves of Bare Au Substrate

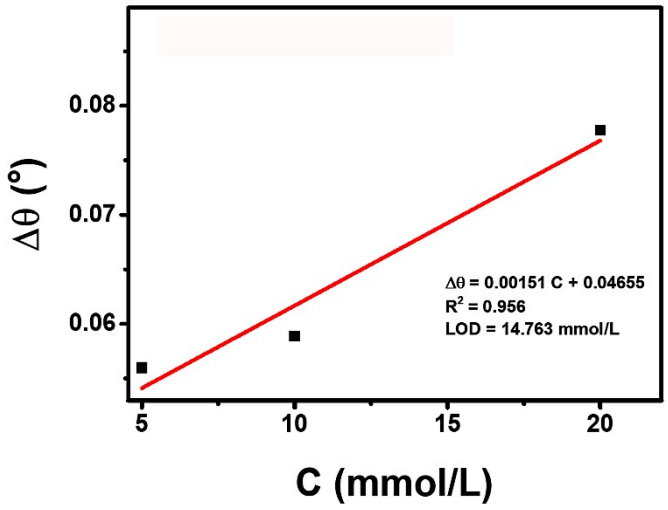

Fig. S4. Calibration curve of the dynamic response of bare Au substrate towards glucose in the concentration range of 5-20 mmol/L (*Δθ vs. C* plot for bare Au substrate).

S5. Selectivity, Reusability, and Stability

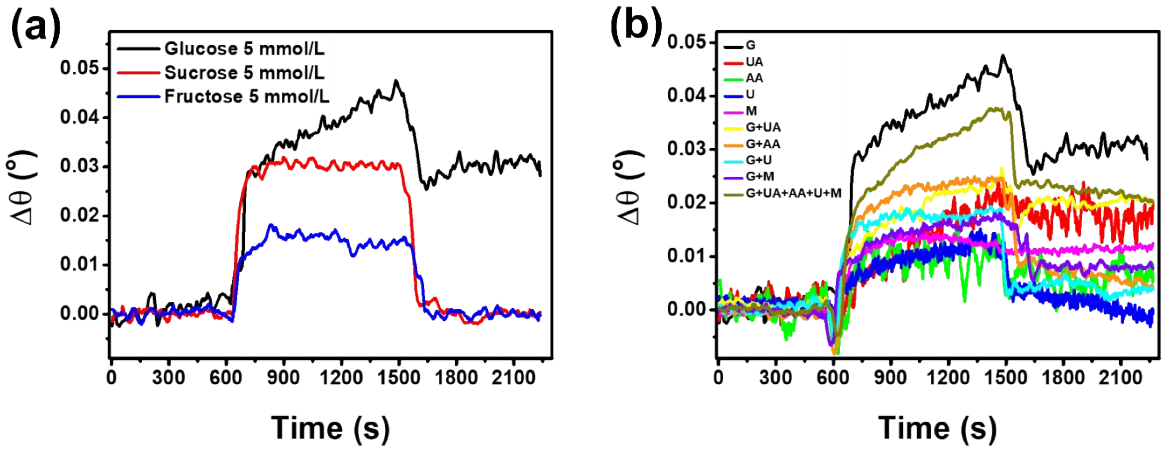

Fig. S5. Selectivity test results: (a) Dynamic responses of the Zr-BDC functionalized SPR sensor towards 5 mmol/L glucose (G), 5 mmol/L sucrose (S), and 5 mmol/L fructose (F). (b) Dynamic responses of the Zr-BDC functionalized SPR sensor towards other competing molecules [0.45 mmol/L uric acid (UA), 0.11 mmol/L ascorbic acid (AA), 5 mmol/L urea (U), and 0.1 mmol/L maltose (M)] and their mixture.

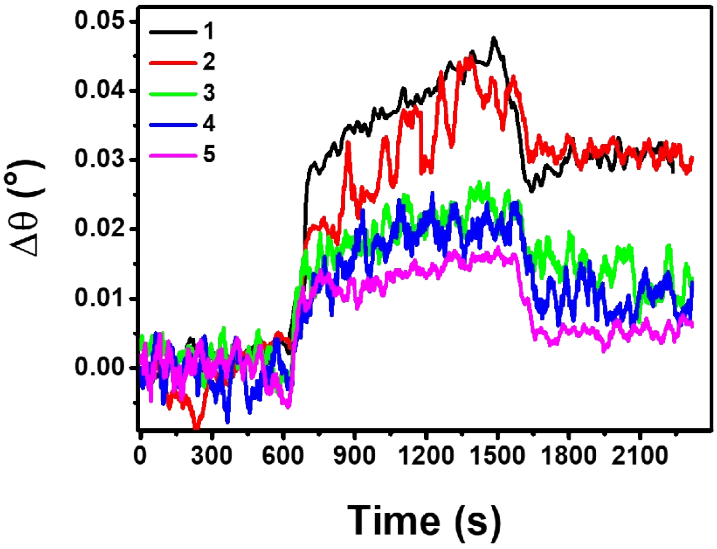

Fig. S6. Reusability test results. Dynamic responses of the Zr-BDC-functionalized SPR sensor to 5 mmol/L glucose from the 1st to 5th measurement.

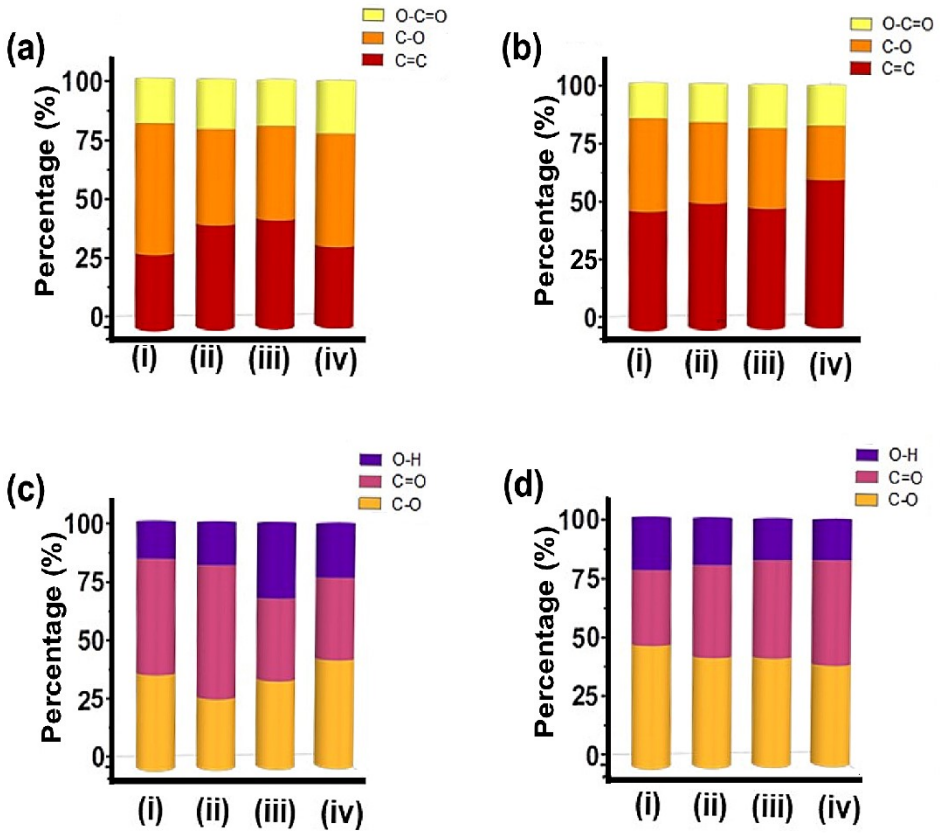

Fig. S7. Atomic percentages of different carbon and oxygen bonds in (i) Zr-BDC, (ii) Mn-BDC (iii) Ni-BDC and (iv) Cu-BDC before (a, b) and after glucose detection (c, d).

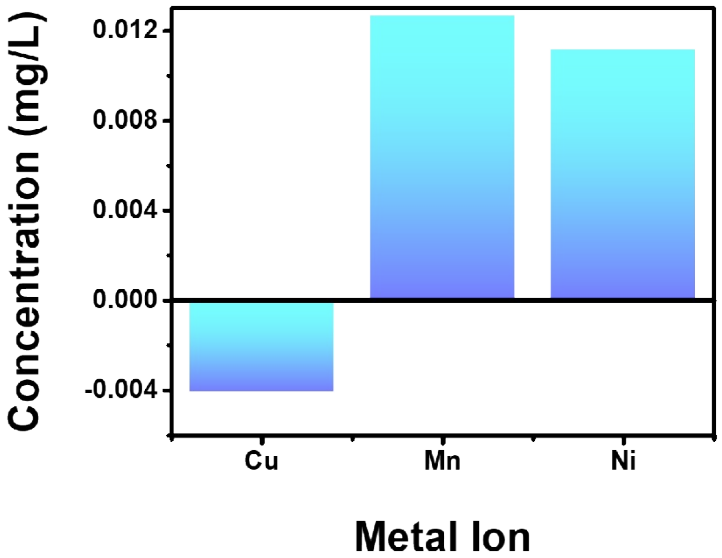

Fig. S8. The concentrations of dissolved metal ions in waste solutions collected after the glucose sensing measurements by Cu-BDC, Mn-BDC, and Ni-BDC, as measured by ICP-OES.

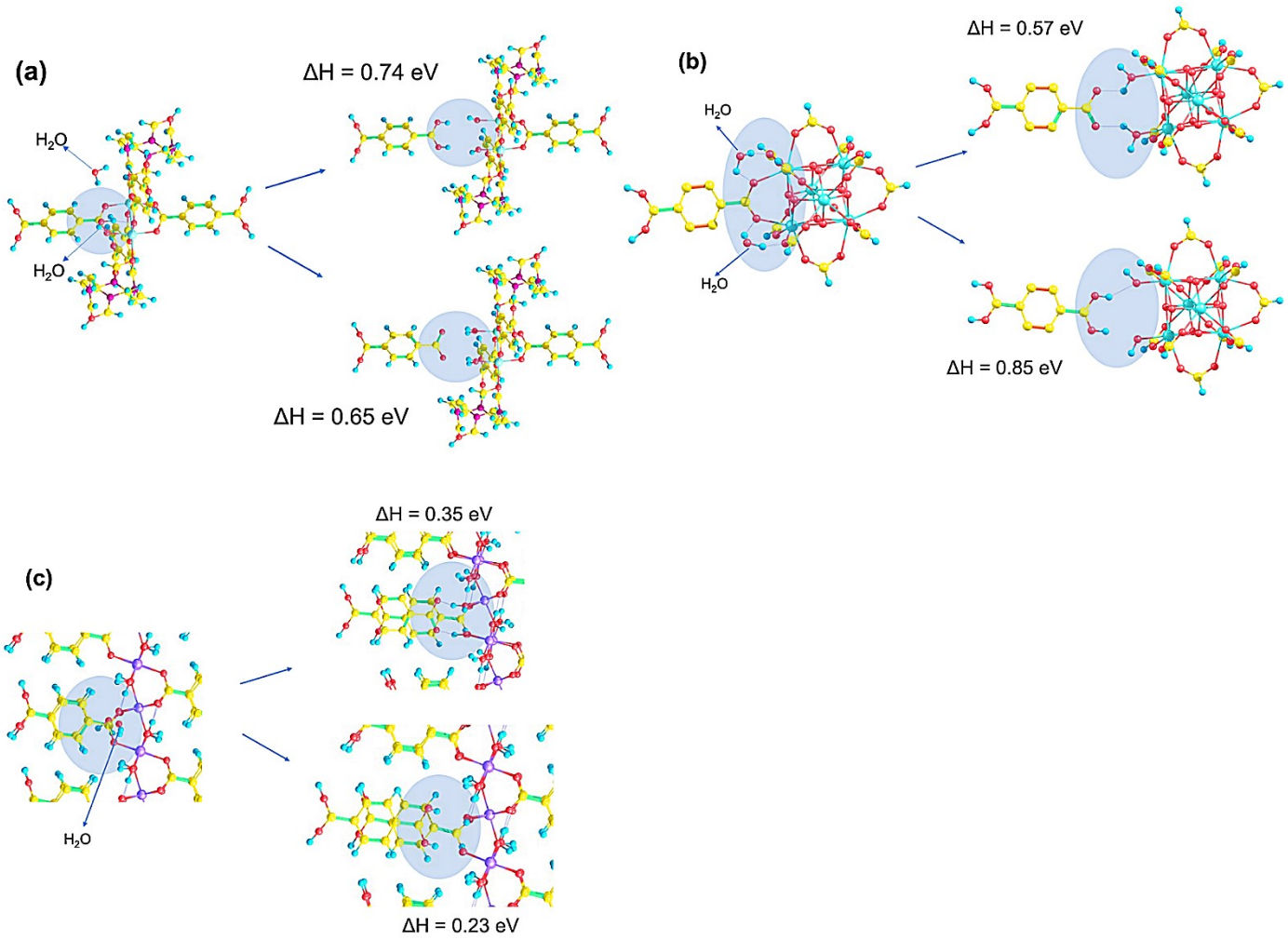

Fig. S9. Schematic of decomposition reaction of M-BDC in the presence of water molecules and their corresponding reaction enthalpies for (a) Cu-BDC, (b) Zr-BDC and (c) Ni-BDC. The yellow, red, and green spheres represent carbon, oxygen and hydrogen atoms, respectively. The turquoise sphere in (a) and (b) represents the Cu and Zr atom, respectively, whereas the purple sphere in (c) represents the Ni atom.

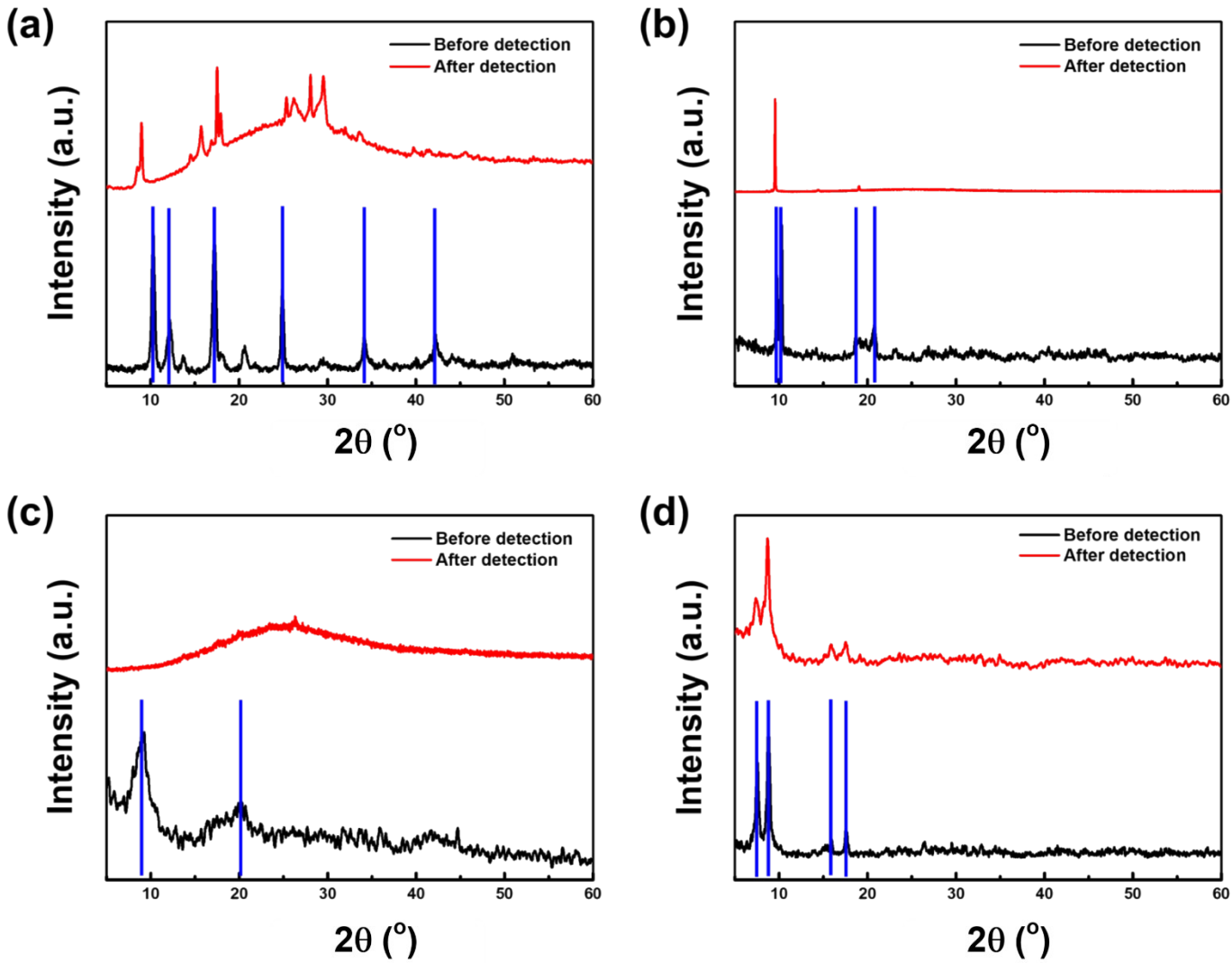

Fig. S10. XRD patterns of (a) Cu-BDC, (b) Mn-BDC, (c) Ni-BDC, and (d) Zr-BDC samples before and after glucose detection.

References

1. G. Gumilar, Y. V. Kaneti, J. Henzie, S. Chatterjee, J. Na, B. Yuliarto, N. Nugraha, A. Patah, A. Bhaumik and Y. Yamauchi, *Chem. Sci.*, 2020, **11**, 3644-3655.
2. A. M. M. Vargas, A. L. Cazetta, M. H. Kunita, T. L. Silva and V. C. Almeida, *Chem. Eng. J.*, 2011, **168**, 722-730.
3. I. S. McLintock, *Nature*, 1967, **216**, 1204-1205.
4. C. Aharoni and M. Ungarish, *J Chem. Soc. Faraday Trans.* , 1976, **72**, 400-408.
5. M. A. Ahmad, N. Ahmad and O. S. Bello, *Appl. Water Sci.*, 2015, **5**, 407-423.
6. A. Göçenoğlu Sarıkaya, B. Osman, T. Çam and A. Denizli, *Sens. Actuators B*, 2017, **251**, 763-772.
7. N. Ayawei, A. N. Ebelegi and D. Wankasi, *J. Chem.*, 2017, **2017**, 3039817.
8. Y. Keren, M. Borisover and N. Bukhanovsky, *Chemosphere*, 2015, **138**, 462-468.
9. M. A. Al-Ghouti and D. A. Da'ana, *J. Hazard. Mater.*, 2020, **393**, 122383.
10. S. Karoui, R. Ben Arfi, K. Mougin, A. Ghorbal, A. A. Assadi and A. Amrane, *J. Hazard. Mater.*, 2020, **387**, 121675.
11. F. Brouers, *J. Mod. Phys.*, 2014, **5**, 1594-1601.
12. F. Brouers and T. J. Al-Musawi, *J. Mol. Liq.*, 2015, **212**, 46-51.